IEEE Access
Multidisciplinary ⋮ Rapid Review ⋮ Open Access Journal

Received September 2, 2020, accepted September 21, 2020, date of publication September 28, 2020,
date of current version October 8, 2020.

Digital Object Identifier 10.1109/ACCESS.2020.3027002

Series Arc Fault Diagnosis and Line Selection Method Based on Recurrent Neural Network

WENCHU LI[1], YANLI LIU[1], YING LI[1], AND FENGYI GUO[2], (Member, IEEE)
[1]Faculty of Electrical and Control Engineering, Liaoning Technical University, Huludao 125105, China
[2]College of Electrical and Electronic Engineering, Wenzhou University, Wenzhou 325035, China

Corresponding author: Fengyi Guo (fyguo64@126.com)

This work was supported in part by the National Natural Science Foundation of China under Grant 52077158 and 51674136, in part by the Liaoning Revitalization Talents Program under Grant XLYC1802110.

ABSTRACT Series arc fault is a common phenomenon in the power system, it will directly affect the working reliability, but there is no mature method to detect it due to its concealment and chaos. Common detection methods that build on the arc fault eigenvectors obtained by manual analysis are subjective and incomprehensive. A series arc fault diagnosis and line selection method based on recurrent neural network (RNN) for a multi-load system was proposed in this paper. Firstly, a series arc fault experiment under a multi-load system was carried out, the training set and test set were built by using the data obtained from the experiment. Then, the RNN model was built, trained, and tested through the training set and test set. Finally, the fast-continuous detection method and the probability-based classification result correction method were proposed, and the detection speed and accuracy were improved much further. The results show that the proposed method is effective for diagnosing series arc fault and line selection under a multi-load system, without analysis of arc fault characteristics.

INDEX TERMS Series arc fault, deep learning, recurrent neural network, RNN, fault diagnosis, fault line selection.

I. INTRODUCTION

Series arc fault often occurs in power supply and distribution systems due to poor contact and other reasons. It may cause electrical fires and even personal injury and death. Owing to its concealment and chaos, there is still a lack of mature detection methods. Parallel asynchronous motors and frequency converters are the main loads in the power supply and distribution system. It will reduce the economic investment of series arc fault detection by realizing the identification of the branch and the phase of the series arc fault, through the current signal of a single phase of the main circuit, under the multi-load situation.

Since the main current and voltage are easy to obtain and hardly interference by the external environment, it is popular that to detect arc fault from current and voltage signals. Various data mining algorithms are used to extract fault features, then the arc fault was detected through classification algorithms, in most studies.

Qiwei Lu proposed a DC series arc fault detection method by using the information on line current and supply voltage [1]. Na Qu uses four features of current in time domain and ten features of current in frequency domain as fault feature [2]. Calderon-Mendoza Edwin extracted fault features through a Kalman filter, then detect arc fault through a Fuzzy logic processor [3]. Shengyang Liu proposed a time and time-frequency domain analysis method combining the loop current and voltage for detecting the series DC arc fault [4]. Nikola L Georgijevic detected arc fault by calculating the modified Tsallis entropy of current [5]. Peiyong Duan used the fast wavelet transform to construct characteristic parameters of the series arc fault [6]. Joshua E Siegel used Fourier coefficients, Mel frequency cepstrum coefficients, and wavelet coefficients as feature quantities to train a neural network for arc fault recognition [7]. Giovanni Artale obtained the characteristics of the arc fault through the Chirp Z Transform (CZT) [8]. Guanghai Bao use current transformer to extract high-frequency components and proposed an arc fault detector based on the microcontroller unit (MCU) [9]. Fengyi Guo comprehensively used wavelet packet theory, variational mode decomposition, and Wigner-Ville distribution to extract the time domain and time-frequency domain characteristics of arc faults, and used particle swarm optimization and grid search optimization

The associate editor coordinating the review of this manuscript and approving it for publication was Youqing Wang.

support vector machines to establish arc fault recognition and selection model [10]. Hongxin Gao used an improved singular value decomposition method to extract arc fault features and used support vector machines (SVM) to identify arc faults [11].

Recurrent neural network (RNN) is one of the deep learning algorithms developed at the beginning of the 21st century. It focuses on sequence input and is widely used in natural language processing, medical diagnosis, and other fields.

Zhe Li used FPGA to realize automatic speech recognition (ASR) based on RNN [12]. Ryota Nishimura proposed a method of searching between different media forms (cross-media mapping) through RNN [13]. Ümit Şentürk combined electrocardiogram (ECG) and photoplethysmography (PPG) signal with RNN and proposed a new hybrid prediction model to continuously estimate blood pressure [14]. Kandarpa Kumar Sarma used RNN as the main method to research vowel phoneme detection, speech recognition, and speech-to-text [15]–[17].

In this paper, a multi-load series arc fault experiment system was built, arc fault diagnosis and line selection experiment under different working conditions was carried out to obtain the main current which was used to build the training set and test set. The RNN model was built, trained, and tested through the training set and test set, which can diagnosis arc fault and select fault line through only one single-phase current of the main circuit. The fast-continuous detection method and probability-based classification result correction method were proposed to further improve the detection speed and accuracy, according to the signal characteristics of the current time-series and the characteristics of the RNN.

Generally, deep learning method is hard to realize on embedded devices, due to its complex network structure, many parameters, and massive calculation. The fast-continuous detection method reduces the amount of calculation and improves the detection speed by modifying the network structure without retraining the network. And the probability-based classification result correction method improve accuracy by evaluating the probability. They can be integrated in the embedded system to realize real-time online detection.

II. SERIES ARC FAULT DIAGNOSIS AND LINE SELECTION EXPERIMENT

A. EXPERIMENTAL SYSTEM AND SCHEME

The main circuit of the experiment system is shown in Fig.1. A 380V three-phase AC power supply drives two parallel three-phase AC asynchronous motors M1 and M2. Among them, M1 is an 11KW motor, and the load current of M1 can be adjusted through a magnetic powder brake, and it can be selected to run with or without the frequency converter. M2 is a 7.5KW motor, running without load. P1-P9 are the access points of the arc fault generator AF, and C1, C2, and C3 are current transformers. The three-phase current data of the main circuit and arc voltage data was saved to the computer through the data acquisition card. And the experimental scheme is shown in Table 1.

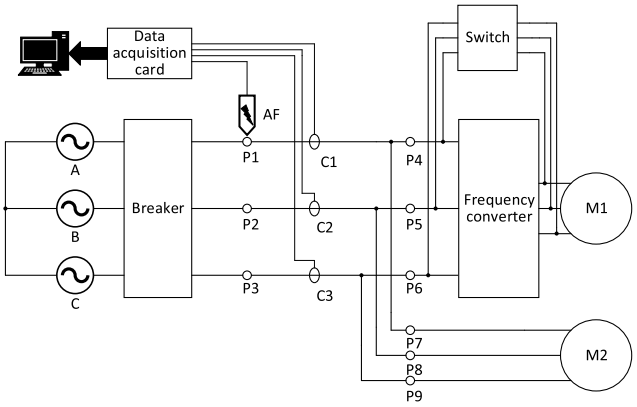

FIGURE 1. The main circuit of the experiment system.

TABLE 1. Experimental scheme.

Group	M1 running status	Frequency converter	M2 running status	Fault point
1−9	No load	off	No load	P1−P9
10−18	17A	off	No load	P1−P9
19−27	20A	off	No load	P1−P9
28−36	17A to 20A	off	No load	P1−P9
37−45	No load	on	No load	P1−P9
46−54	17A	on	No load	P1−P9
55−63	20A	on	No load	P1−P9
64−72	17A to 20A	on	No load	P1−P9

M1 with frequency converter and magnetic powder brake, M2, experimental circuit, and AF which developed according to the GB14287 standard are shown in Fig.2(a), Fig.2(b), Fig.2(c), and Fig.2(d), respectively.

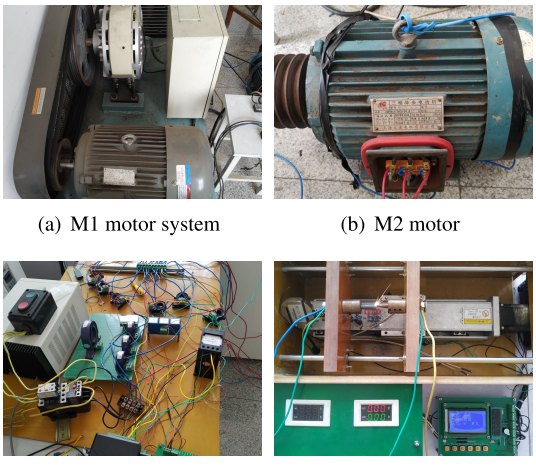

(a) M1 motor system (b) M2 motor

(c) Experimental circuit (d) Arc fault generator

FIGURE 2. Experimental setup.

B. ANALYSIS OF EXPERIMENTAL RESULTS

In the case of the P4 point (phase A of the M1 branch) fails and the M1 runs without the frequency converter, the main current is shown in Fig.3. Comparing Phase A and Phase B current while the P4 point fails with the normal current in Fig.3(a), it can be found that at the same time, the currents of both phase A and phase B have obvious spike noise signals, but the amplitude of phase B is a little bigger than that of phase A, indicating that an arc fault occurs in one phase can be reflected in the current signals of other phases. And comparing with the three-phase current in Fig.3(b), it can be found that the noise signal caused by the arc fault is shown in all three-phase of the current and occurred at the same time.

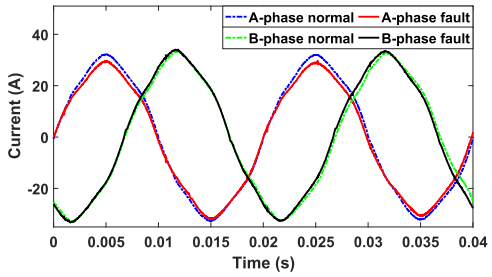

(a) Phase A and Phase B current under P4 fault without frequency converter compared with normal state

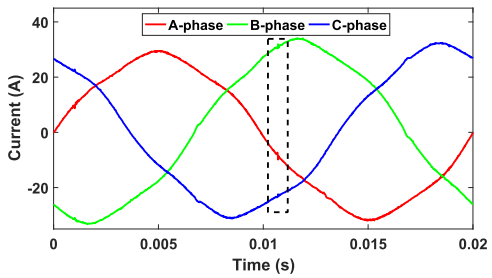

(b) Three-phase current under P4 fault without frequency converter

FIGURE 3. The main current waveform under P4 fault without frequency converter compared with normal state.

In the case of the P4 point fails and the M1 runs with the frequency converter, the main current waveform is shown in Fig.4. It can be seen that there is little difference in the amplitude of the double- peaks of the current waveform during normal state. When an arc fault occurs in phase A, both amplitude of the double-peak of the fault phase decreases, and the amplitude difference between the double-peaks increases. In the other two phases, the amplitude difference between the double-peaks also increases, but both amplitude of the double-peak increases compared with the normal state. And through comparison, it is found that the amplitude increases of phase C, the leading phase of the fault phase, is greater than the amplitude increases of phase B, the lagging phase of the fault phase.

In the case of the P1 point (phase A of the main circuit) fails and the M1 runs with the frequency converter, the main

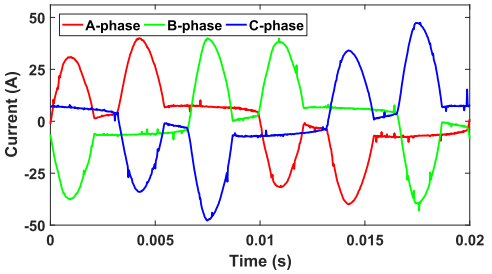

(a) Three-phase normal current with frequency converter

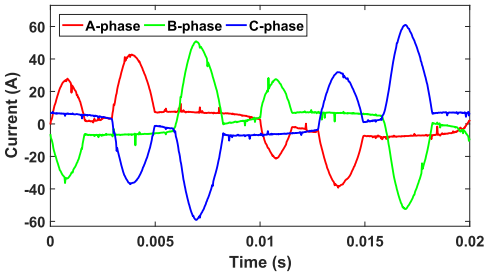

(b) Three-phase current under P4 fault with frequency converter

FIGURE 4. The main current waveform P4 fault with frequency converter compared with normal state.

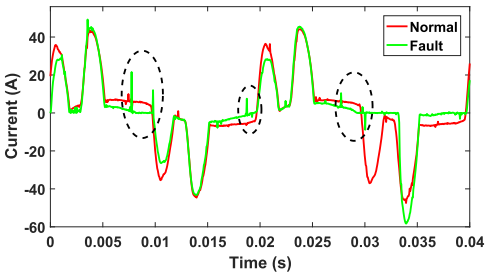

(a) Phase A current under P1 fault with frequency converter

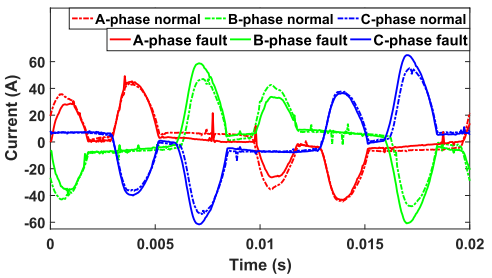

(b) Three-phase current under P1 fault with frequency converter compared with normal state

FIGURE 5. The main current waveform under P1 fault with frequency converter compared with normal state.

current is shown in Fig.5. It can be seen that the amplitude of all three-phase current changes. And the fault characteristics appear as a superposition of the fault characteristics of both two branches, due to its the main circuit fault. And there has been an increase of harmonic content in all three phases, but

the most in the fault phase. However, faults like single-phase grounding may also lead to an increase in the harmonic content of a certain phase of the power supply system. It is not scientific enough to use only the harmonic content as a diagnostic basis for the phase of the arc fault.

In summary, there are some patterns caused by arc fault in the main current waveform, but it is relatively and not obvious, thus it is difficult to judge by logic or threshold. Therefore, the diagnosis and line selection model can be established through deep learning.

III. THE ESTABLISHMENT OF SERIES ARC FAULT DIAGNOSIS AND LINE SELECTION MODEL

Joshua E Siegel pointed out that the current signal can be played in the form of audio to distinguish arc fault [7]. It means that arc faults can be diagnosed through the audio processing method. Recurrent neural network (RNN) has a wide range of applications in audio recognition processing and other fields. In this paper, the advantage of RNN to be good at processing time-series data was taken to establish the arc fault diagnosis and line selection model.

A. ESTABLISHMENT OF SAMPLE LIBRARY

A neural network must be trained with enough data. The sample library was built using the data obtained from the experiment. Only one single-phase current of main circuit should be used to detect the arc fault, but all three phases current of main circuit were recorded in the experiment. It is obviously that the phase A current when an arc fault occurs on phase A should have the same fault characteristics with the phase B current when an arc fault occurs on phase B, under the same working condition, due to the symmetry of the three-phase circuit. They should be regarded as the same kind of fault, the measured phase fault. Therefore, by using the concept of relative phase, the current of all three phases can be used to train the neural network, which increased the number of samples significantly. There are ten kinds of labels were given in Table.2.

TABLE 2. Fault type label.

Fault type	Label value
Measured phase main circuit fault	0
Measured phase M1 branch fault	1
Measured phase M2 branch fault	2
Leading phase main circuit fault	3
Leading phase M1 branch fault	4
Leading phase M2 branch fault	5
Lag phase main circuit fault	6
Lag phase M1 branch fault	7
Lag phase M2 branch fault	8
Normal	9

The sample library was built with 50289 samples. Each sample contains 784 sampling points, about one period. 45,260 samples were randomly selected and built as the training set, and the remaining 5029 samples were built as the test set.

To improve the accuracy and convergence speed of the model, it is necessary to normalize the samples. The standard deviation was used to normalize the sample data.

B. THE ESTABLISHMENT OF THE RECURRENT NEURAL NETWORK

The recurrent neural network (RNN) is usually used to describe sequence data. It currently has more successful applications in speech recognition, natural language processing, medical diagnosis, and other fields.

The RNN model used in this paper was built with 2 recurrent layers and three full connect layers. The detail of the model structure is shown in Table.3.

TABLE 3. RNN model structure.

Layer type	Number of Nodes	Number of Parameters	RNN architecture	Activation function	Output size
FC	128	3712	-	None	28×128
RNN	128	32896	Many to many	tanh	28×128
FC	64	8256	-	None	28×64
RNN	64	8256	Many to one	tanh	64
FC	10	650	-	softmax	10

The unfolded diagram of the RNN structure is shown in Fig.6. The forward propagation calculation process of this network is shown in Fig.7.

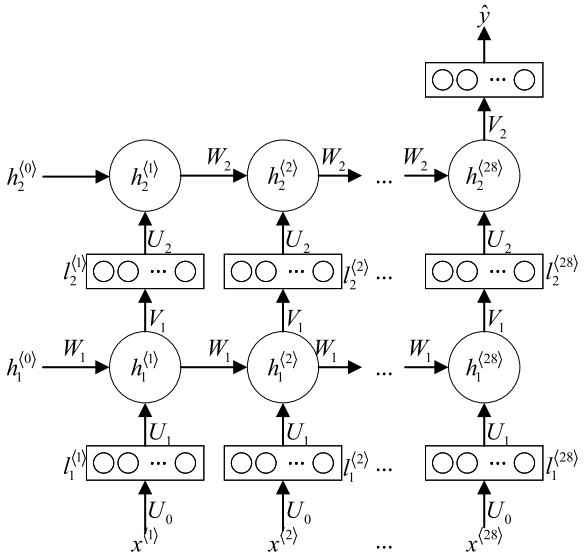

FIGURE 6. The proposed RNN structure diagram.

The bias vectors and activation functions are omitted in the unfolded diagram, among them, U_0, U_1, U_2, V_1, V_2, W_1, W_2, are all neural network coefficient matrices, and b_0 to b_4 are the bias vectors. Both the coefficient matrices and the bias vectors are obtained by training the network. The input

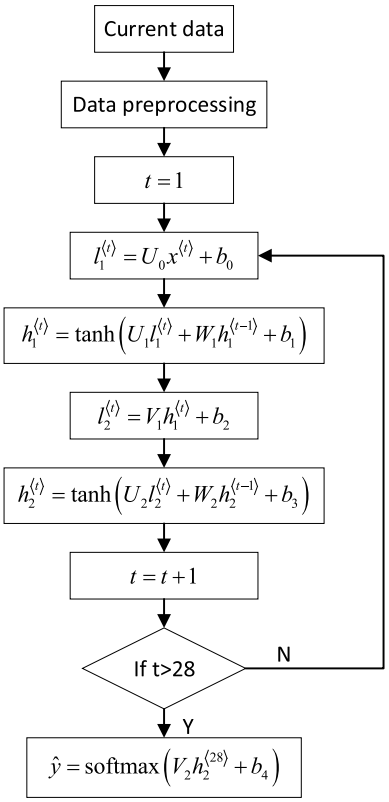

FIGURE 7. The proposed RNN forward propagation flow chart.

sample data is cut into 28 segments $x^{<1>}$ to $x^{<28>}$, which are the inputs of the RNN. $l_1^{<t>}$ and $l_2^{<t>}$ are the values of hidden nodes of full connect layers at t-period. $h_1^{<t>}$ and $h_2^{<t>}$ are the values of hidden nodes of recurrent layers at t-period. Among them, $h_1^{<0>}$ and $h_2^{<0>}$, both zero vectors, are the initial values of the recurrent units. Finally, the classification result $\hat{y}$ is obtained after 28 periods of calculation. $\hat{y}$ is a 10×1 column vector, the 10 values of $\hat{y}$ represent the network's estimate of the probability of 10 possible outcomes, respectively. The outcomes with the maximum probability will be the classification results of the network.

C. RNN TRAINING AND TESTING

To train the RNN, it is necessary to measure the difference between the true value and the estimated value of the RNN output by using the loss function. The cross-entropy function was selected as the loss function of the proposed RNN model, see (1).

$$loss(Y, \hat{Y}) = -\sum_{i=1}^{N}\sum_{j=1}^{M} y_{ij} \times log\hat{y}_{ij} \tag{1}$$

In (1), Y is the true value, $\hat{Y}$ is the estimated value. N is the number of samples, M is the number of labels, y_{ij} is the indicator variable (0 or 1), $\hat{y}_{ij}$ is the probability that sample i belongs to category j.

The optimizer optimizes the neural network by adjusting the network parameters to minimize the loss function. Adam was used as the optimizer. It's an algorithm for first-order gradient-based optimization of stochastic objective functions, based on adaptive estimates of lower-order moments. The method is straight forward to implement, is computationally efficient, has little memory requirements, is invariant to diagonal rescaling of the gradients, and is well suited for problems that are large in terms of data and/or parameters. The method is also appropriate for non-stationary objectives and problems with very noisy and/or sparse gradients. The hyper-parameters have intuitive interpretation sand typically require little tuning [18].

The network was trained 200 epochs, with a batch size of 256, by using TensorFlow, and tested through both the training set and test set. The accuracy and loss of the network are shown in Fig.8.

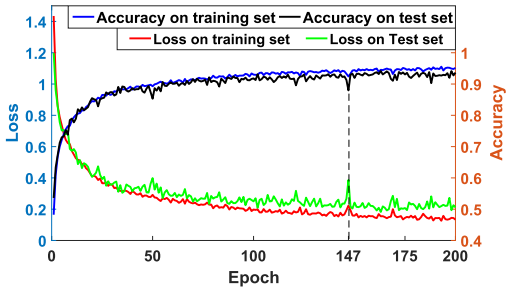

FIGURE 8. Accuracy and loss of the RNN.

Comparing the changes in the accuracy and the loss value, it is found that the accuracy increases rapidly in the first 25 epochs of training, and the corresponding loss value decreases rapidly. Subsequently, the increase in accuracy tended to be flat, and finally remained at about 94%.

At the 147th epoch of training, it can be seen that the accuracy of the network has decreased significantly, on both the test set and the training set. And the corresponding loss value has also increased. Since the Adam algorithm is essentially RMSprop with momentum term, it was guessed that the momentum term tries to jump out of the trap by increasing the update amplitude when the loss value oscillates locally, but the overall training process is relatively stable and the convergence is relatively rapid.

After the 175th epoch, although the test results have a little growth on the training set, and remain within a certain range on the test set, and fluctuate without significant growth. Therefore, to prevent the network from over fitting, the training should be stopped and the exported network model should be saved.

IV. THE IMPROVEMENT OF SERIES ARC FAULT DIAGNOSIS AND LINE SELECTION MODEL

In this section, the fast-continuous detection method and probability-based classification result correction method

were proposed to further improve the detection speed and accuracy.

A. FAST-CONTINUOUS DETECTION METHOD

Both training and testing use fixed-length data and $h^{<0>}$ are zero vectors of the unimproved RNN proposed in section III. It outputs one classification result after every 28 periods, which has a large amount of calculation and slow detection.

The network structure is modified, to increase the speed and reduce the quantity of calculation. The second recurrent layer was changed from many-to-one to many-to-many, and the restriction on sequence length was removed, on the foundation of keeping the coefficient matrices and the bias vectors unchanged. By this way, the network will give a result after every 28-sampling points input, continuously. The structure of improved RNN is shown in Fig.9.

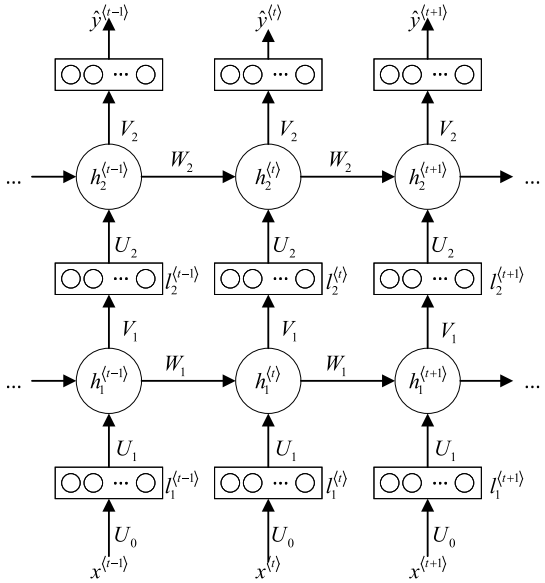

FIGURE 9. Improved RNN structure diagram.

It is hard for RNN to memorize the characteristics of longer data sequences. The output result at a certain moment is affected by the results of the previous moments, and the influence decrease as the time interval increases. Therefore, increasing the number of cycles will have little impact on the output results, so that the network can perform rapid real-time detection of continuous long sequences.

B. PROBABILITY-BASED CLASSIFICATION RESULT CORRECTION METHOD

Comparing the output classification result of the improved RNN with its corresponding probability, it is found that when the network has misjudgment, the corresponding probability will be relatively reduced. The latest classification result can be corrected, according to the probability and historical classification results. The final diagnosis and line selection model is shown in Fig.10, which consists of two parts: an

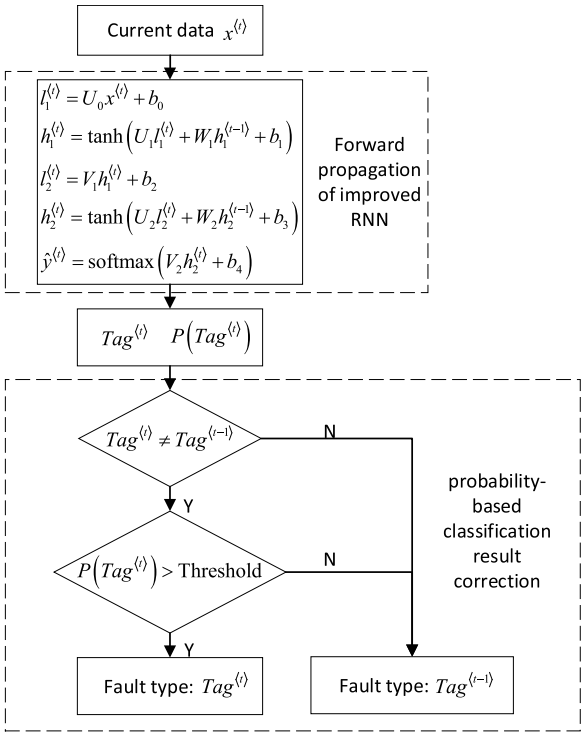

FIGURE 10. Improved diagnosis and line selection model.

improved RNN and a probability-based classification result correction.

Given the input data $x^{<t>}$ in the t-period, the label value $Tag^{<t>}$ and the corresponding probability $P(Tag^{<t>})$ can be obtained through the improved RNN. Then Judge and correct RNN classification result based on probability and historical results. Only when the probability corresponding to the label is high enough (bigger than the Threshold) will the classification result of the improved RNN be accepted, otherwise the classification result of the previous period will be used as an alternative.

C. THE TEST OF THE IMPROVED DIAGNOSIS AND LINE SELECTION MODEL

Three complete and continuous current time-series data of different fault types are input into the improved diagnosis and line selection model, the duration of all three pieces of data is 15 seconds, and the continuous results output is shown in Fig.11. The right vertical axis is the classification label value output by the improved RNN (the blue points) and the probability-based classification result correction (the red X points). The corresponding relationship between the label value and the fault type is shown in Table.2. The left vertical axis is the probability corresponding to the classification label value, and the horizontal axis is time. In Fig.11(a), it can be seen that an arc fault occurs around 9.2 seconds, classification results of 9 between 0 seconds and 9.2 seconds indicate that no fault has occurred, and classification results of 0 between 9.2 seconds and 15 seconds indicate the measured phase

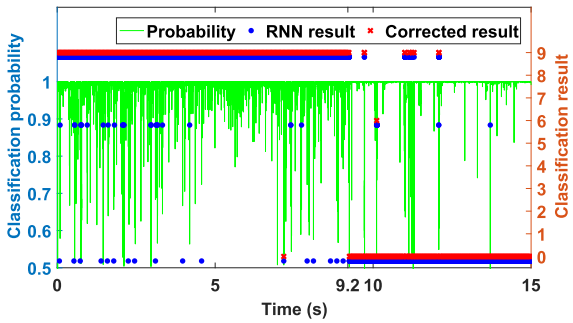

(a) Measured phase main circuit fault

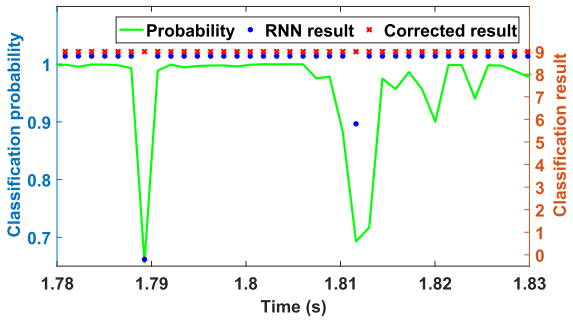

(b) Partially enlarged of (a)

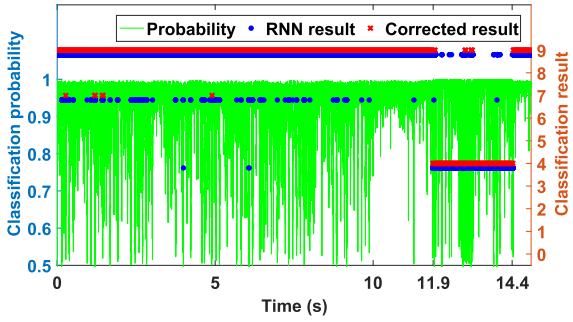

(c) Leading phase M1 branch fault

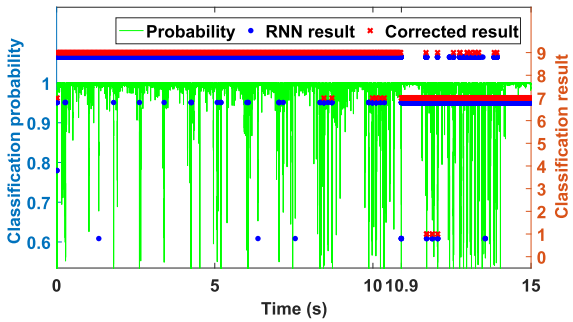

(d) Lag phase M1 branch fault

FIGURE 11. The test of Improved diagnostic and line selection model.

main circuit fault. In Fig.11(c), it can be seen that the fault occurred around 11.9 seconds, and the fault label value is 4, which belongs to the leading phase M1 branch fault then the fault disappears around 14.4 seconds. The system returns to normal. In Fig.11(d), it can be seen that a fault occurs near 10.9 seconds and the fault label value is 7, which belongs to the lag phase M1 branch fault.

It can be seen that there are still misjudgment points in the results of the RNN improved by the fast-continuous detection method as shown by the blue isolated points in Fig.11. The improved RNN has an accuracy of 97.6% for continuous long-term current sequence, which is better than the unimproved RNN tested by random fragment data from the test set. It is also found that there are more misjudgment points at the beginning of detecting and before the arcing, but they are relatively isolated. It is guessed that these two kinds of misjudgments are mainly caused by too little input data, and the increase in contact resistance before the contacts are completely separated, respectively.

Zoom in Fig.11(a) from 1.78 seconds to 1.83 seconds to obtain Fig.11(b). It has two misjudgment points from the results of the improved RNN. Both misjudgment points have a low probability. By using the probability-based classification result correction method the misjudgment points were easily fixed (the red X points).

Comparing the results of improved RNN and probability-based classification result correction in Fig.11, the accuracy of the latter is significantly higher, which reached 98.7%.

D. THE REALIZE OF THE PROPOSED METHOD IN REAL-WORLD RUNNING SYSTEMS

The method proposed in this paper is programmed by Python with the support of TensorFlow and runs on a computer. There are two ways to realize it in a real-world running system.

1) Run the network on a Raspberry Pi which is a Linux based micro-computer that can run Python code and TensorFlow directly. Through the Raspberry Pi the proposed method can be easily embedded into the real-world running systems with slight modification.
2) The proposed method can also runs on a DSP or an ARM chip like STM32. Since DSP and ARM can not run TensorFlow directly, the Python code based on TensorFlow should be rewritten in C language follow the flow chart shown in Fig.10. The flash and ROM of DSP and ARM may be not enough for network parameters, therefore external storage is necessary.

The realizing on a DSP or ARM system of the proposed method is recommended, due to its stability and reliability in industrial applications, even if it is more complicated.

V. CONCLUSION

In this paper, series arc fault experiment under a multi-load system was carried out, then a series arc fault diagnosis and line selection method based on recurrent neural network (RNN) for the multi-load system was proposed. The proposed method can also be used in other fields to realize series arc fault diagnosis and line selection, with appropriate modification and enough training data. The conclusions are as follows:

1) In a multi-motor parallel system, whether it is a series arc fault in the motor branch or the main circuit, the main current will be distorted, but in different degrees of the fault phase and normal phases.
2) By training the RNN with signal phase main current data under different working conditions, series arc fault diagnosis and line selection can be realized, which has an accuracy of 94%, but without characteristic analysis of the current signal.
3) The proposed fast-continuous detection method and probability-based classification result correction method can effectively improve the accuracy and speed of diagnosis and line selection model with an accuracy of 98.7%.

ACKNOWLEDGMENT

The authors would like to thank the reviewers for their many constructive comments.

REFERENCES

[1] Q. Lu, Z. Ye, M. Su, Y. Li, Y. Sun, and H. Huang, "A DC series arc fault detection method using line current and supply voltage," *IEEE Access*, vol. 8, pp. 10134–10146, 2020.
[2] N. Qu, J. Zuo, J. Chen, and Z. Li, "Series arc fault detection of indoor power distribution system based on LVQ-NN and PSO-SVM," *IEEE Access*, vol. 7, pp. 184020–184028, 2019.
[3] E. Calderon-Mendoza, P. Schweitzer, and S. Weber, "Kalman filter and a fuzzy logic processor for series arcing fault detection in a home electrical network," *Int. J. Elect. Power Energy Syst.*, vol. 107, pp. 251–263, May 2019.
[4] S. Liu, L. Dong, X. Liao, X. Cao, X. Wang, and B. Wang, "Application of the variational mode decomposition-based time and time–frequency domain analysis on series DC arc fault detection of photovoltaic arrays," *IEEE Access*, vol. 7, pp. 126177–126190, 2019.
[5] N. L. Georgijevic, M. V. Jankovic, S. Srdic, and Z. Radakovic, "The detection of series arc fault in photovoltaic systems based on the arc current entropy," *IEEE Trans. Power Electron.*, vol. 31, no. 8, pp. 5917–5930, Aug. 2016.
[6] P. Duan, L. Xu, X. Ding, C. Ning, and C. Duan, "An arc fault diagnostic method for low voltage lines using the difference of wavelet coefficients," in *Proc. 9th IEEE Conf. Ind. Electron. Appl.*, Jun. 2014, pp. 401–405.
[7] J. E. Siegel, S. Pratt, Y. Sun, and S. E. Sarma, "Real-time deep neural networks for Internet-enabled arc-fault detection," *Eng. Appl. Artif. Intell.*, vol. 74, pp. 35–42, Sep. 2018.
[8] G. Artale, A. Cataliotti, V. Cosentino, D. Di Cara, S. Nuccio, and G. Tine, "Arc fault detection method based on CZT low-frequency harmonic current analysis," *IEEE Trans. Instrum. Meas.*, vol. 66, no. 5, pp. 888–896, May 2017.
[9] G. Bao, R. Jiang, and X. Gao, "Novel series arc fault detector using high-frequency coupling analysis and multi-indicator algorithm," *IEEE Access*, vol. 7, pp. 92161–92170, 2019.
[10] F. Guo, H. Gao, Z. Wang, J. You, A. Tang, and Y. Zhang, "Detection and line selection of series arc fault in multi-load circuit," *IEEE Trans. Plasma Sci.*, vol. 47, no. 11, pp. 5089–5098, Nov. 2019.
[11] H. Gao, X. Wang, T. Nguyen, F. Guo, Z. Wang, J. You, and Y. Deng, "Research on feature of series arc fault based on improved SVD," in *Proc. IEEE Holm Conf. Electr. Contacts*, Sep. 2017, pp. 325–331.
[12] Z. Li, C. Ding, S. Wang, W. Wen, Y. Zhuo, C. Liu, Q. Qiu, W. Xu, X. Lin, X. Qian, and Y. Wang, "E-RNN: Design optimization for efficient recurrent neural networks in FPGAs," in *Proc. IEEE Int. Symp. High Perform. Comput. Archit. (HPCA)*, Feb. 2019, pp. 69–80.
[13] R. Nishimura, M. Higaki, and N. Kitaoka, "Mapping acoustic vector space and document vector space by RNN-LSTM," in *Proc. IEEE 7th Global Conf. Consum. Electron. (GCCE)*, Oct. 2018, pp. 329–330.
[14] Ü. Şentürk, I. Yücedağ, and K. Polat, "Repetitive neural network (RNN) based blood pressure estimation using PPG and ECG signals," in *Proc. 2nd Int. Symp. Multidisciplinary Stud. Innov. Technol. (ISMSIT)*, Oct. 2018, pp. 1–4.
[15] K. Dutta and K. K. Sarma, "Multiple feature extraction for RNN-based assamese speech recognition for speech to text conversion application," in *Proc. Int. Conf. Commun., Devices Intell. Syst. (CODIS)*, Dec. 2012, pp. 600–603.
[16] M. Sharma and K. K. Sarma, "Dialectal assamese vowel speech detection using acoustic phonetic features, KNN and RNN," in *Proc. 2nd Int. Conf. Signal Process. Integr. Netw. (SPIN)*, Feb. 2015, pp. 674–678.
[17] K. Dutta and K. K. Sarma, "Dynamic segmentation of vocal extract for assamese speech to text conversion using RNN," in *Proc. 2nd Nat. Conf. Comput. Intell. Signal Process. (CISP)*, Mar. 2012, pp. 126–131.
[18] D. P. Kingma and J. Ba, "Adam: A method for stochastic optimization," *Comput. Sci.*, 2014.

WENCHU LI was born in Liaoyang, Liaoning, China, in 1995. He received the B.S. degree from Liaoning Technical University, Huludao, China, in 2017, where he is currently pursuing the M.S. degree. His current research interests include electrical contact theory and arc.

YANLI LIU was born in Liaoning, China, in 1981. She received the B.S., M.S., and Ph.D. degrees in electrical engineering from Liaoning Technical University, in 2004, 2007, and 2017, respectively.

She is currently an Associate Professor with Liaoning Technical University. She has published more than 20 articles. Her current research interests include electrical contact theory and arc.

YING LI was born in Liaoning, China, in 1981. She received the B.S. and M.S. degrees from the Faculty of Electrical and Control Engineering, Liaoning Technical University, Huludao, China, in 2004 and 2007, respectively, where she is currently pursuing the Ph.D. degree. Her current research interests include electrical contact theory and arc.

FENGYI GUO (Member, IEEE) was born in Chifeng, China, in 1964. He received the B.S. and M.S. degrees from the Fuxin Mining Institute, Fuxin, China, in 1987 and 1990, respectively, and the Ph.D. degree from Xi'an Jiaotong University, Xi'an, China, in 1997, all in electrical engineering.

He was a Visiting Professor with the University of Pretoria, Pretoria, South Africa, from 2002 to 2003, and with the University of Oxford, Oxford, U.K., from 2008 to 2009. He is currently a Professor of electrical engineering with Wenzhou University, Wenzhou, China. He has published more than 150 articles. His current research interests include electrical contact, arc, and intelligent apparatus.